Published in final edited form as:
Dev Cell. 2007 May ; 12(5): 727–738. doi:10.1016/j.devcel.2007.02.011.

aPKC controls microtubule organization to balance adherens junction symmetry and planar polarity during development

Tony J. C. Harris[1,2,*] and **Mark Peifer**[2,3]

[1]Department of Cell and Systems Biology, University of Toronto, Toronto, ON M5S 3G5, Canada

[2]Department of Biology, University of North Carolina at Chapel Hill, Chapel Hill, NC 27599-3280, USA

[3]Lineberger Comprehensive Cancer Center, University of North Carolina at Chapel Hill, Chapel Hill, NC 27599-3280, USA

Summary

Tissue morphogenesis requires assembling and disassembling individual cell-cell contacts without losing epithelial integrity. This requires dynamic control of adherens junction (AJ) positioning around the apical domain, but the mechanisms involved are unclear. We show that atypical Protein Kinase C (aPKC) is required for symmetric AJ positioning during *Drosophila* embryogenesis. aPKC is dispensable for initial apical AJ recruitment, but without aPKC, AJs form atypical planar-polarized puncta at gastrulation. Preceding this, microtubules fail to dissociate from centrosomes, and at gastrulation, abnormally persistent centrosomal microtubule asters cluster AJs into the puncta. Dynein enrichment at the puncta suggests it may draw AJs and microtubules together and microtubule disruption disperses the puncta. Through cytoskeletal disruption in wildtype embryos, we find a balance of microtubule and actin interactions controls AJ symmetry versus planar polarity during normal gastrulation. aPKC apparently regulates this balance. Without aPKC, abnormally strong microtubule interactions break AJ symmetry and epithelial structure is lost.

Introduction

Proper assembly and maintenance of tissue and organ architecture are critical for normal development and homeostasis. Epithelia are the most common animal tissue architecture, forming sheets of adherent cells that act as boundaries between our body compartments. Loss of proper epithelial architecture is a hallmark of many late stage cancers. Epithelial structure is normally maintained by adherens junctions (AJs), in which homophilically interacting cadherin receptors link to cytoplasmic β-catenin (fly Armadillo; Arm) and α-catenin (Gumbiner, 2005; Jamora and Fuchs, 2002; Nelson, 2003; Tepass et al., 2001). AJs interact with the actin and microtubule (MT) cytoskeletons, forming a dynamic protein interaction network that controls epithelial structure.

All cells are polarized, and establishment of apical-basal polarity is critical for epithelial tissue architecture in all animals. In *Drosophila*, apical-basal polarity is established during

*Correspondence: Tony Harris, Dept. of Cell and Systems Biology, Univ. of Toronto, 25 Harbord St., Toronto, ON M5S 3G5, Canada. Tel: (416) 946-0873. Fax: (416)978-8532. tony.harris@utoronto.ca.

cellularization, when Bazooka (Baz)/PAR-3 directs apical assembly of AJs (Fehon, 2006). This initial polarity is then elaborated by the polarized accumulation and action of other polarity complexes, which mutually interact to reinforce apical-basal polarity.

After polarity establishment, epithelial morphogenesis begins. This introduces a third dimension, as cells move in the plane of the epithelium and the first evidence of planar polarity emerges. AJs are normally symmetrically distributed around the apex of each epithelial cell, adhering neighboring cells to maintain epithelial structure (Gumbiner, 2005; Jamora and Fuchs, 2002; Nelson, 2003; Tepass et al., 2001). However, epithelial morphogenesis requires cells to exchange neighbors and this requires asymmetric AJ assembly events. For example, new contacts and new AJs must form between intercalating cells as they meet during convergent extension (Bertet et al., 2004; Blankenship et al., 2006; Irvine and Wieschaus, 1994; Zallen and Wieschaus, 2004).

Similarly, as epithelial cells divide, they maintain AJs with their neighbors and asymmetrically assemble a new contact between the daughter cells (Knox and Brown, 2002). However, AJ symmetry must be restored or maintained for proper epithelial structure. Thus specific regulatory mechanisms must exist to balance transient asymmetric AJ assembly events and overall AJ symmetry, but the mechanisms regulating this are unknown.

Proteins of the PAR-3/PAR-6/aPKC complex regulate cellular symmetry in many contexts, controlling polarity from *C. elegans* embryos to mammalian neurons and stem cells (Kemphues, 2000; Munro, 2006; Nance, 2005; Wiggin et al., 2005; Wodarz, 2005). In epithelia, these polarity regulators control AJ assembly and maintenance in the apical domain (Nelson, 2003; Ohno, 2001; Tepass et al., 2001). In *Drosophila*, mutants lacking core AJ components lose epithelial structure as epithelial rearrangements are initiated at gastrulation (Cox et al., 1996; Harris and Peifer, 2004; Muller and Wieschaus, 1996). Bazooka (Baz)/PAR-3 is required for the polarized assembly of cadherins into AJs and *baz* mutants also fail at gastrulation (Harris and Peifer, 2004; Muller and Wieschaus, 1996). Although Baz/PAR-3 often functions in a complex with aPKC and PAR-6, in the early *Drosophila* epithelium Baz co-localizes with AJs while aPKC and PAR-6 localize apical to Baz (Harris and Peifer, 2005). This suggests that aPKC and PAR-6 may have distinct functions from Baz. While Baz is essential for initial assembly of AJs, Par-6 appears to maintain them at gastrulation (Hutterer et al., 2004). aPKC plays an important role in the polarity of neural cells at larval stages (Rolls et al., 2003), but the role of aPKC in establishment and elaboration of polarity in *Drosophila* embryogenesis has not been determined. Here, we report that aPKC is not critical for the initial establishment of polarity but that it plays a unique role in regulating AJ symmetry around the apical domain during gastrulation, convergent extension and later development.

Results

aPKC is dispensable for polarity establishment but promotes AJ symmetry

Zygotic aPKC mutants survive embryogenesis, presumably due to the maternal contribution, and die as larvae with neuronal defects (Rolls et al., 2003). To assess aPKC's embryonic role, we examined embryos maternally and zygotically mutant for the null *apkc*^{k06403} allele (Rolls et al., 2003). *apkc*$^{m/z}$ mutants form the cellular blastoderm epithelium normally. In contrast to mutants affecting Baz or AJ proteins (Cox et al., 1996; Harris and Peifer, 2004; Muller and Wieschaus, 1996), we found that *apkc*$^{m/z}$ mutants gastrulate, forming a ventral furrow and posterior midgut invagination (Figure 1A, B). Relative to wildtype (WT; Figure 1C, D), gastrulating *apkc*$^{m/z}$ mutants display disorganized epithelial cell shape and positioning, but do not lose overall epithelial structure as occurs in the absence of Baz or AJs (Cox et al., 1996; Harris and Peifer, 2004; Muller and Wieschaus, 1996; Figure 1E, F). *apkc*$^{m/z}$ mutants also undergo convergent extension, shifting the posterior germband anteriorly over the dorsal

surface of the embryo (Figure 1G). However, at full germband extension, *apkc*$^{m/z}$ mutants undergo widespread epithelial cell dissociation (Figure 1G; compare with WT, Figure 1H; also see Figure 2O, P). Both *apkc*$^{m/z}$ mutants and paternally-rescued *apkc*^{m} mutants (with zygotic aPKC expression) die as embryos, and their remaining epithelia secrete only scraps of cuticle (Figure 1I, vs. WT with an intact cuticle, Figure 1J). Thus, the ectoderm can form and undergo initial morphogenesis in *apkc*$^{m/z}$ mutants, but epithelial structure is progressively lost during development.

We next examined the cell biological consequences of loss of aPKC on establishment and subsequent elaboration of apical-basal polarity. Polarity is initiated by apical localization of Baz and AJ proteins during cellularization, forming discontinuous, but symmetrically distributed, spot junctions (Figure 2A, C), which subsequently coalesce into continuous belt junctions around the apex of each epithelial cell (Figure 2E, G) during germ band extension (Harris and Peifer, 2004; Tepass and Hartenstein, 1994). In *apkc*$^{m/z}$ mutant cellular blastoderms, AJs initially assemble at the normal apical position (Harris and Peifer, 2005), and AJs (labeled by *Drosophila* E-Cadherin; DE-Cad) and Baz colocalize in symmetrically distributed spot junctions (Figure 2B), as in WT (Figure 2A).

In WT embryos, DE-Cad and Baz continue to colocalize in symmetrically distributed spot junctions during early gastrulation (Harris and Peifer, 2004; Tepass and Hartenstein, 1994). In contrast, as *apkc*$^{m/z}$ mutants begin gastrulation (after ventral furrow formation but before germ band extension), the spot junctions coalesce into abnormal single puncta centrally placed on the dorsal and ventral edges of each ectodermal epithelial cell (Figure 2D; DE-Cad is slightly less enriched in the puncta, retaining a low level even cortical distribution). These asymmetrical DE-Cad and Baz puncta form a planar-polarized pattern over the surface of gastrulating *apkc*$^{m/z}$ mutants (Figure 2J), in contrast to the symmetrical spot junctions seen in WT (Figure 2I). The AJ protein Arm follows its binding partner DE-Cad, localizing with Baz in the planar-polarized puncta (Figure 3A; similar to DE-Cad, Arm is less enriched than Baz), while WT Arm is evenly distributed in spot junctions (Figure 3B). During posterior midgut invagination and early germband extension, WT embryos begin to form relatively symmetrical belt junctions (Figure 2E), while in *apkc*$^{m/z}$ mutants the planar-polarized AJ/Baz puncta persist (Figure 2F).

Spot junctions form in their normal apical location in *apkc*$^{m/z}$ mutants (Harris and Peifer, 2005), and like WT spot junctions (Figure 2K), the planar-polarized puncta remain apical during early gastrulation (Figure 2L; mutant puncta localize between 1.5 +/-0.4 and 4.6+/-0.8 μm below the embryo surface, as measured in groups of >10 ectodermal cells of five embryos from five experiments; WT spot junctions localize between 1.2 +/-0.4 and 4.5+/-1.4 μm below the embryo surface (n=5)). During germband extension, WT belt junctions are repositioned to the apex of cell-cell contacts (Harris and Peifer, 2005; Figure 2M), but the puncta in *apkc*$^{m/z}$ mutants fail to do so, remaining more basal along the lateral membrane (Figure 2N). At the end of germband extension, AJs and Baz remain in puncta in *apkc*$^{m/z}$ mutants, but these become randomly positioned along both the apical-basal and planar axes (Figure 2H, P; contrast with symmetrical WT junctions, Figure 2G, O), and epithelial architecture is lost as cells dissociate or cluster in small groups. The transition in *apkc*$^{m/z}$ mutants from AJ/Baz symmetry at cellularization, to planar polarized AJ/Baz puncta at gastrulation, to randomly positioned AJ/Baz puncta following germband extension appears to be fully penetrant, being observed in >20 separate experiments.

The formation of abnormal AJ/Baz puncta in *apkc*$^{m/z}$ mutants reveals a critical role for aPKC in maintaining AJ symmetry during gastrulation and later development. The fact that AJ/Baz puncta first arise as an ordered planar polarized array, suggested that they form due to a relatively specific defect in AJ positioning in *apkc*$^{m/z}$ mutants. To test this hypothesis, we examined the localization of other polarity regulators.

aPKC is important for polarity maintenance and elaboration

After apical-basal polarity establishment during cellularization, other polarity proteins localize asymmetrically and help elaborate the initial polarization (Bilder et al., 2003; Hutterer et al., 2004; Tanentzapf and Tepass, 2003). We thus examined the localization of other polarity proteins in *apkc*$^{m/z}$ mutants. In WT embryos, both the Baz/aPKC-binding partner PAR-6 (Figure 3D, F) and the apical determinant Crumbs (Fig. 3H, J) become enriched at the apical cortex as gastrulation begins. In aPKC mutants, neither PAR-6 (Figure 3C, E) nor Crumbs (Figure 3G, I) become enriched in the Baz/AJ puncta; instead both are largely lost from the cortex. We also analyzed the restriction of Discs Large (Dlg), a component of the basolateral Dlg/Lethal Giant Larvae (Lgl)/ Scribble complex, to the basolateral membrane. During gastrulation, Dlg is not excluded from theapical domain in either WT or *apkc*$^{m/z}$ mutants (Figure 3K, L, arrows point to Dlg accumulations of apical surface membrane). However, in WT, Dlg is excluded from the apical domain by the end of gastrulation (Figure 3N), but remains apical during the later epithelial breakdown in *apkc*$^{m/z}$ mutants (Figure 3M, arrow). Thus aPKC is dispensable for polarity establishment but does play important roles in subsequent epithelial cell polarity maintenance/elaboration.

aPKC inhibits AJ-microtubule interactions

These effects on polarity elaboration, while striking, cannot easily account for the early focusing of AJs into planar polarized puncta in *apkc*$^{m/z}$ mutants. One mechanism that might regulate AJ positioning is cytoskeletal association. To test whether the asymmetric AJ positioning in *apkc*$^{m/z}$ mutants involves alterations in actin or MTs, we examined cytoskeletal organization. WT actin is relatively evenly distributed around the apical cell periphery with considerable overlap with spot junctions and enrichment at tri-cellular junctions (Figure 4B). In *apkc*$^{m/z}$ mutants, actin accumulates at tri-cellular junctions (Figure 4A) more than in WT (Figure 4B), but actin is not obviously enriched in Baz puncta. Similarly, during the later epithelial breakdown in *apkc*$^{m/z}$ mutants, actin is not specifically enriched at fragmented AJs (Figure 4C); in contrast WT belt junctions are closely underlain by actin (Figure 4D). The lack of actin enrichment at the early puncta in *apkc*$^{m/z}$ mutants may partially explain the failure to maintain symmetrical spot AJs. The altered actin localization might be a downstream consequence of mislocalized Baz/AJ complexes, and/or it might affect the puncta through lateral exclusion. However, we sought to identify a clustering mechanism acting directly at the puncta.

We next examined MTs. MT-based apical transport helps initially position AJ/Baz complexes (Harris and Peifer, 2005). In WT, duplicated centrosomes localize apical to the nuclei in the same apical-basal plane as Baz/AJ complexes, while MTs form bundles running down the lateral membrane. However, at this stage, the MT bundles display minimal centrosomal association (Figure 4F; bundles in cross-section, arrowheads), and although their sides are in close proximity to AJs, they do not precisely colocalize (Figure 4F, arrowheads).

In contrast, MTs have a strikingly abnormal organization in *apkc*$^{m/z}$ mutants, displaying a very specific association with the AJ/Baz puncta (Figure 4E). In *apkc*$^{m/z}$ mutants MT asters emanate from the apical centrosomes, and both are closely associated with AJ/Baz puncta—one of the two centrosomes typically associates with the puncta at the dorsal side of the cell while the other associates with the puncta on the ventral side (Figure 4E, arrows). Thus, asters from two neighboring cells often appear on either side of a single puncta (Figure 4E, inset), suggesting that the AJ/Baz complexes bridge the two cells, presumably via cadherin interactions (in 7 embryos from 7 experiments, 184/200 AJ/Baz puncta associated with abnormal MT asters, and 36.7 +/-3.5% of the puncta had an aster on both sides). Close associations between AJs and centrosomal MTs are also found as epithelia disintegrate in *apkc*$^{m/z}$ mutants (Figure 4G), in

contrast to WT (Figure 4H), suggesting that abnormal AJ-MT interactions may continue to inhibit AJ symmetry during epithelial breakdown.

Since similar MT asters are not seen at either stage in WT embryos (e.g., Figure 4F), one mechanism that could explain the atypical AJ/Baz puncta is prolonged or enhanced MT-centrosome association in *apkc*$^{m/z}$ mutants. Alternately, the abnormal MT-centrosome associations could be a secondary consequence of AJ disruption. To test this, we examined gastrulation stage *arm*$^{m/z}$ mutants that lack AJs. Neither residual epithelial cells nor dissociated cells display the abnormal MT asters observed in *apkc*$^{m/z}$ mutant cells (Harris and Peifer, 2004; Figure S2). *arm*$^{m/z}$ mutants do display abnormal MT organization but it is distinct from the *apkc*$^{m/z}$ mutant phenotype, indicating that the abnormal MT organization in *apkc*$^{m/z}$ mutants cannot be solely attributed to AJ disruption and that aPKC likely has more direct affects on MTs. To assess how aPKC could affect AJ-MT interactions, we compared the localization of aPKC and MTs in the apical domain in WT. During cellularization, early gastrulation and germband extension, aPKC is enriched at the cortex, with some localization in the cytoplasm, but without specific colocalization with MTs (Fig 4, I-K). Thus, aPKC could affect MTs at the cortex or in the cytoplasm.

aPKC blocks MT-centrosome association during cellularization

Our results suggested that aPKC might play an early role in regulating MT-centrosome interactions during *Drosophila* development. To test this mechanistic hypothesis, we first evaluated WT MT organization in the cellular blastoderm, just before the onset of gastrulation. During cellularization the first epithelium forms—invaginations of embryo surface membrane simultaneously compartmentalize several thousand nuclei into individual columnar cells (Nelson, 2003). During cellularization, MTs were reported to emanate from apical centrosomes and run down and past the invaginating lateral membranes to form inverted MT baskets over each nucleus (Warn and Warn, 1986). Since our analyses indicate that WT MTs show little centrosome association at gastrulation, we wondered when MT-centrosome interactions are normally disrupted. To address this, we imaged living WT embryos injected with rhodamine-labeled Tubulin, focusing on the most apical plane in which MTs were visible. At the beginning of cellularization, two prominent MT asters are found at the apical end of each cell compartment (Figure 5A, 0:00). During mid-late cellularization these asters begin to fragment (Figure 5A, 0:21), and by the end of cellularization apical MTs are mainly organized into separate bundles running down the lateral membrane (Figure 5A; 0:29; individual MT bundles are seen in cross section). We observed similar results in embryos expressing Tubulin-GFP (Figure S1), and also used this analysis to confirm the 3D-relationships of MT asters and bundles at each stage by imaging at different apical-basal planes. The fragmentation of MT bundles from the centrosomes was observed in live imaging of 11 embryos. Imaging of fixed embryos also revealed MT-centrosome associations early in cellularization (Figure 5B; apical MT asters were observed in 17/19 embryos from 3 experiments) and their loss by the end of cellularization (Figure 5C; apical MT asters were absent in 12/12 embryos from 3 experiments). As the top of each inverted MT basket splinters away from the centrosomes, MTs become more symmetrically distributed around the apical domain. Thus during WT cellularization, MTs are re-organized so that most apical MTs lose colocalization with the two apical centrosomes and become symmetrically distributed as part of MT bundles running down the sides of each cell (Figure 5D; 5H shows side view).

We hypothesized that aPKC regulates MT organization during cellularization. To test this we examined cellularizing *apkc*$^{m/z}$ mutants. In early cellularization apical MTs are centrosome-associated (Figure 5E; apical MT asters were observed in 22/22 embryos from 6 experiments) as in WT (Figure 5B). However, in *apkc*$^{m/z}$ mutants MTs fail to dissociate from centrosomes at the end of cellularization, and prominent centrosome-associated MT asters persist (Figure

5F; 5I is a side view; apical MT asters were observed in 10/10 embryos from 6 experiments), in contrast to WT (Figure 5C, H). The effect of aPKC on apical MT organization is relatively specific, as MTs emanating from the centrosomal asters in *apkc*$^{m/z}$ mutants can form lateral bundles running down the sides of each cell (Figure 5G, I), as in WT (Figure 5D, H). Moreover, *apkc*$^{m/z}$ mutants have normal mitotic spindles during prior syncytial nuclear divisions and later epithelial cell divisions (data not shown). Importantly, the abnormal apical MT organization in *apkc*$^{m/z}$ mutants arises before gross defects in AJ/Baz positioning. Thus, aPKC appears to play an early role in regulating apical MT organization, triggering MT-centrosome dissociation and a more symmetric MT distribution around the apical domain as cellularization ends.

Persistent microtubule interactions and the loss of AJ symmetry

We previously found that Dynein functions in the initial apical positioning of AJs and Baz during cellularization (Harris and Peifer, 2005). Since Dynein can link AJs to MTs (Ligon et al., 2001), and also functions in positioning centrosomes centrally within the cell (Gomes et al., 2005), we hypothesized that AJs and centrosomes may be drawn together in gastrulating *apkc*$^{m/z}$ mutants by cortical Dynein. To examine this potential mechanism, we evaluated Dynein localization. During gastrulation, Dynein heavy chain localizes evenly around the cortex and in the cytoplasm of both WT (Figure 6A) and *apkc*$^{m/z}$ mutant (Figure 6B) embryos. Dynein intermediate chain displays a similar localization (Figure 6C). At the end of WT germband extension, Dynein heavy chain continues to localize evenly around the cortex and cytoplasmically (Figure 6D). However, at the end of *apkc*$^{m/z}$ mutant germband extension, Dynein heavy chain becomes noticeably enriched at the AJ fragments (Figure 6E). Similarly, Dynein intermediate chain is enriched at these AJ fragments (Figure 6F). The presence of Dynein at these sites is consistent with a role in maintaining the abnormal associations between AJs and centrosomal MTs associated with later epithelial breakdown in *apkc*$^{m/z}$ mutants. Although Dynein has a more even cortical distribution during gastrulation, it is possible that Dynein could also function in the early formation of the puncta.

To test whether persistent association with MTs and centrosomes may be the mechanism drawing AJs and Baz into planar-polarized puncta in *apkc*$^{m/z}$ mutants, we examined whether disruption of MT asters disperses the AJ/Baz puncta. We first assessed AJ and Baz positioning in mutant epithelial cells undergoing their first cell division at the end of gastrulation. In these cells, as MTs are reorganized to form mitotic spindles, the abnormal MT asters associated with AJ/Baz puncta disassemble (Figure 6G, dividing cells, right (outlined); those yet to divide, left). As abnormal cortical MT asters are lost, DE-Cad and Baz become more evenly distributed around the cell periphery (Figure 6G, brackets), compared with neighboring cells yet to divide (Figure 6G, arrows; observed in 8/8 embryos; DE-Cad shows greater dispersion from the original puncta). To further test whether MTs stabilize the abnormal AJ/Baz puncta, we treated gastrulating *apkc*$^{m/z}$ mutants with colchicine to disrupt MTs. In regions with residual MTs, planar-polarized DE-Cad/Baz puncta are retained (Figure 6H, arrows), but in neighboring regions without detectable MTs, DE-Cad and Baz formed smaller puncta distributed evenly around the full cell periphery (Figure 6H, brackets; observed in 9/9 embryos). Mock treatment has no effect (Figure 6I; no effect in 4/4 embryos). Thus, persistent MT associations provide a possible mechanistic explanation for the loss of AJ symmetry in *apkc*$^{m/z}$ mutants.

A balance of interactions with actin and microtubules regulates junctional symmetry versus planar polarity

These data suggest the possibility that cytoskeletal interactions like those perturbed in *apkc*$^{m/z}$ mutants may regulate normal planar polarity. To test whether cytoskeletal interactions regulate AJ positioning during normal development, we treated WT embryos with cytoskeletal inhibitors for 30 min and examined the effects on AJs and Baz (in these experiments Baz and DE-Cad were imaged by deconvolution of confocal stacks of the full apical region and are

shown as projections revealing all apical Baz and DE-Cad). With this analysis, Baz planar polarity becomes quite evident in untreated control embryos by the onset of germband extension (Figure 7B, arrows; stages 7-8)), as reported previously (Zallen and Wieschaus, 2004; there may be subtle planar polarity during early gastrulation before germband elongation (late stage 6); Fig 7A; recent quantitation by Blankenship et al. 2006 suggests this is the case). However, in contrast to *apkc*$^{m/z}$ mutants WT Baz enrichment occurs along the full length of dorsal-ventral cell-cell contacts rather than being restricted to tight puncta, and AJs remain relatively symmetrically distributed. When we treated with colchicine to disrupt MTs, we observed minimal effects on Baz and AJ positioning at gastrulation and germband extension (Figure 7C, D; there may be a subtle increase in localization to tricellular junctions at gastrulation).

Reasoning that a balance of cytoskeletal interactions might control planar-polarized Baz/AJ positioning, we examined the role of the actin cytoskeleton. To test the effects disrupting actin, we treated with cytochalasin D. This resulted in a striking enhancement of the planar polarization of both Baz and AJs; both were now dramatically planar-polarized before the onset of germband extension (Figure 7E, arrows), and were hyperpolarized after the onset of germband extension (Figure 7F, arrows). This suggests that actin acts early to restrain junctional asymmetry. To further probe possible roles of MTs, we simultaneously treated embryos with both cytochalasin D and colchicine. This largely reversed the effects on inhibiting actin alone, restoring a more symmetric distribution of Baz and AJs (Figure 7G, H). To quantify these results we measured the relative fluorescence intensity at dorsal-ventral (DV) versus anterior-posterior (AP) contacts averaging the ratios from five cells per embryo and measuring three stage 7-8 embryos per experiment. In control embryos, Baz and DE-Cad displayed DV-AP ratios of 2.82±0.56 and 1.42±0.14, respectively. With cytochalasin D, Baz and DE-Cad displayed significantly higher DV-AP ratios of 7.06±0.20 and 4.11±0.14, respectively (T tests, $p<0.001$). With cytochalasin D plus colchicine, Baz and DE-Cad displayed DV-AP ratios lower than controls, 1.00±0.31 and 1.25±0.14, respectively. Similarly, with colchicine alone, Baz and DE-Cad displayed DV-AP ratios lower or equal to controls, 1.89±0.30 and 1.46±0.23. These results suggest that MTs contribute to the enhanced Baz/AJ planar polarity resulting from actin disruption and that a balance between MT and actin interactions normally maintains AJ symmetry. In *apkc*$^{m/z}$ mutants, the abnormal persistence of apical MT asters appears to disrupt this balance leading to planar polarized AJ clustering (Figure 7I).

Discussion

Our study provides the first view of the roles of aPKC during polarity establishment and elaboration in *Drosophila* embryos. In contrast to *C. elegans* (Tabuse et al., 1998), aPKC is not critical during initial polarity establishment, as Baz and AJs are initially localized correctly and the embryonic epithelium can undergo initial morphogenesis. However, aPKC plays an early and striking role in maintaining the symmetrical organization of AJs, via effects on MT organization, and also plays an important later role in the elaboration of polarity.

aPKC's later role in polarity elaboration may reflect effects on multiple targets. We found that aPKC is critical for the cortical localization of its normal binding partner PAR-6 and the apical determinant Crb. This latter effect is consistent with the fact that aPKC can phosphorylate Crb and disruption of aPKC phosphorylation sites in Crb destabilizes Crb in the apical domain (Sotillos et al., 2004). Since Crb stabilizes AJs after gastrulation (Tepass, 1996), this likely contributes to the eventual AJ breakdown in *apkc*$^{m/z}$ mutants. Crb may act in concert with PAR-6 (Lemmers et al., 2004) or in parallel. aPKC can also phosphorylate and exclude the basolateral cue Lgl from the apical domain (Hutterer et al., 2004), and we observed failure to exclude Dlg from the apical domain in *apkc*$^{m/z}$ mutants. Thus, apical invasion of basolateral cues may also contribute to the eventual loss of epithelial polarity in *apkc*$^{m/z}$ mutants.

However, it is unlikely that these global changes in apical-basal cell polarity are responsible for the early clustering of AJs into planar polarized puncta in *apkc*$^{m/z}$ mutants. Indeed, most of these other polarity players affect polarity after gastrulation. *crb* mutants have normal spot junctions during gastrulation and early germband extension (Tepass, 1996). Lgl and Dlg are not normally excluded from the apical domain until after gastrulation (Harris and Peifer, 2004; Hutterer et al., 2004). Similarly, while mammalian aPKC can restrict PAR-1 to the basolateral domain of epithelial cells (Hurov et al., 2004), *Drosophila* PAR-1 is not normally excluded from the apical domain at gastrulation (Bayraktar et al., 2006). Thus, effects on Crb, Lgl/Dlg and PAR-1 cannot easily account for the focusing of AJs and Baz into discrete planar polarized puncta as *apkc*$^{m/z}$ mutants gastrulate.

Instead, our data suggest that aPKC regulates AJ symmetry by regulating MTs. MT regulation may be a common aPKC function. For example, *Drosophila* aPKC promotes MT stability at synaptic boutons of neuromuscular junctions, where aPKC forms a complex with Futsch (a MAP1B-like protein) and Tubulin, recruiting Futsch to boutons to stabilize MTs (Ruiz-Canada et al., 2004). aPKC also regulates MT orientation as mammalian astrocytes and fibroblasts undergo directed migration during wound healing (Cau and Hall, 2005; Etienne-Manneville and Hall, 2003), while in MDCK cells, aPKC helps organize the MT cytoskeleton during ciliogenesis (Fan et al., 2004).

MT organization and reorganization play important roles in epithelial morphogenesis, and our data demonstrate that loss of aPKC disrupts these events. During *Drosophila* cellularization, strong MT nucleation from apical centrosomes is likely necessary for assembling lateral MTs that support the apical transport of lipids and proteins to form cell membranes (Lecuit and Wieschaus, 2000; Papoulas et al., 2005). These MTs also help direct the initial apical positioning of AJs and Baz (Harris and Peifer, 2005). During later development, our analysis of *apkc*$^{m/z}$ mutants indicates that centrosomal MTs can effect the symmetric positioning of AJ around the apical domain. Without aPKC activity, the centrosomes become abnormally dominant, bipolar cues, directing AJ clustering and thus disrupting AJ symmetry. Although this abnormal MT organization differs from changes to MT organization observed in AJ mutants (Harris and Peifer, 2004; Figure S2), we cannot rule out the possibility that there is feedback between MTs and AJs during epithelial morphogenesis and that aPKC may regulate these interactions. Indeed, such feedback is very likely and it will be critical to define MT-AJ cross talk mechanisms in future studies.

In *apkc*$^{m/z}$ mutants, MT-associated AJ/Baz puncta assemble at the dorsal and ventral sides of the cells (Figure 2), where new cell-cell contacts form as cells intercalate for the convergent extension of the germ band (Bertet et al., 2004;Blankenship et al., 2006;Irvine and Wieschaus, 1994;Zallen and Wieschaus, 2004). This suggests that MTs may normally function in AJ assembly at these newly formed cell-cell contacts. However, these polarized AJ assembly events must also be counterbalanced to maintain AJ symmetry and proper epithelial structure. Our cytoskeletal inhibitor studies suggest that AJ symmetry may normally be regulated by a balance of MT-AJ and actin-AJ interactions at this stage—actin appears to counteract MT-based AJ assembly at dorsal and ventral cell contacts (Figure 7). Actin was recently shown to be enriched at anterior and posterior cell contacts, suggesting that it may be an early planar polarity cue at this stage (Blankenship et al., 2006). Perhaps this planar polarized actin stabilizes a pool of AJs at anterior and posterior cell contacts, thereby counterbalancing MT-based AJ assembly at dorsal and ventral contacts. Alternatively, lower levels of actin at dorsal and ventral cell contacts could directly counteract MT-based AJ assembly at these sites. Distinguishing these possibilities requires further study. Nonetheless, the *apkc*$^{m/z}$ mutant phenotype appears to arise from a gain-of-function effect in which MTs become overactive and the proper balance between MT-AJ and actin-AJ interactions is lost. As a result, there is a break in AJ symmetry

in *apkc*$^{m/z}$ mutants, MT-associated AJ puncta eventually become randomly positioned, and the epithelium dissociates (Figure 7I).

Our data suggest a speculative mechanistic model by which aPKC could normally regulate MT-AJ interactions. We show that MT association is responsible for the abnormal AJ asymmetry seen in *apkc*$^{m/z}$ mutants, and that Dynein accumulates at these abnormal AJ/Baz puncta. Since Dynein plays a role in apical transport of AJ/Baz proteins during cellularization (Harris and Peifer, 2005), we propose that aPKC may normally regulate release of AJ/Baz complexes from Dynein, allowing a complete transport cycle. In the absence of this release, AJ/Baz complexes could maintain an abnormal association with MTs and localized Dynein activity may pull the centrosomes and spot junctions together into the abnormal puncta seen in *apkc*$^{m/z}$ mutants. This abnormal cortical Dynein activity might also stabilize MTs emanating from the centrosomes, resulting in the persistent centrosomal MTs in the mutants. Alternatively, aPKC may function at the centrosomes to decrease MT nucleation or increase MT severing. Future experiments will illuminate these mechanisms and the generality of aPKC's role in controlling MT organization and AJ positioning.

Experimental Procedures

Fly stocks and genetics—FlyBase describes mutations and constructs (http://flybase.bio.indiana.edu). *apkc*^{K06403} m/z mutants were made by the FLP dominant female-sterile method as done previously (Harris and Peifer, 2005). WT was *yellow white*. *apkc*^{K06403} flies were a gift of C. Doe (Univ. Oregon).

Embryo staining and treatment—For tubulin and KLP10a, embryos were fixed in 10:9:1 heptane:37% formaldehyde:0.5M EGTA for 10 min. For other staining, embryos were fixed for 20 min in 1:1 3.7% formaldehyde in PBS:heptane. After methanol devitellinization, blocking and staining was in PBS/1% goat serum/0.1% Triton X-100. Antibodies were: mouse mAbs against Arm (1:500), Crb (1:500; Developmental Studies Hybridoma Bank (DSHB)), Dlg (1:100; DSHB), Dynein intermediate chain (1:500; Covance), γ-tubulin (1:350; Sigma), tubulin (1:100; DSHB), rabbit pAbs against Baz (1:2000; A. Wodarz, Univ. Dusseldorf, Germany), Dynein heavy chain (1:500; T. Hays, Univ. Minnesota) Klp10a (1:1000; S. Rogers, Univ. North Carolina), ζ PKC (1:2000; Santa Cruz) and rat mAbs against DE-Cad (1:100; T. Uemura, Kyoto Univ., Japan), PAR-6 (1:100; C. Doe, Univ. Oregon). Colchicine and cytochalasin D treatments were performed as described previously (Harris and Peifer, 2005).

Image acquisition, quantification and manipulation—Fixed embryos were mounted in Aqua Polymount (Polysciences, Inc.), and imaged with a 510 confocal microscope (Carl Zeiss MicroImaging, Inc.), at RT, with both 40x (Plan-NeoFluor; NA 1.3) and 63x (Plan-Apochromat; NA 1.4) objectives, and LSM 510 AIM software. Secondary Abs were Alexa 488, 546 and 647 (Molecular Probes). Image deconvolution and projections were done using Velocity software (Improvision). Fluorescence intensity measurements were taken using Image J software (NIH) from projections of deconvolved confocal stacks. The average fluorescence intensity was measured for 12 pixel diameter circles at a clear dorsal-ventral and anterior-posterior contact, and in the cytoplasm for each cell. The measurement from the cytoplasm was subtracted from each cell contact measurement, and the background-corrected dorsal-ventral measurement was divided by the background-corrected anterior-posterior measurement to quantify the enrichment at the dorsal-ventral cell contact relative to the anterior-posterior contact. Unless otherwise noted, Adobe Photoshop 6.0 was used to adjust input levels so the main range of signals spanned the entire output grayscale, and was used to adjust brightness and contrast. We used bicubic interpolation for image re-sizing, but observed no changes to the data at normal viewing magnifications.

Time-lapse microscopy—Dechorionated WT embryos were placed in halocarbon oil (series 700; Halocarbon Products Corporation) and mounted on a gas-permeable membrane (petriPERM; Sigma). For embryos injected with rhodamine-labeled tubulin (Cytoskeleton), images were captured every 10 s with a Wallac Ultraview Confocal Imaging System (PerkinElmer), at RT, with a 40x (Nikon Pan Fluor, N.A. 1.30) objective, an ORCA-ER digital camera (Hamamatsu) and Metamorph Software. For tubulin-GFP embryos, images were collected every 0.5 sec (3 sec per stack) with a Quorum spinning disk confocal system (Quorum Technologies), at RT, with a 63x (Plan-Apochromat; NA 1.4) objective and Volocity software.

Supplementary Material

Refer to Web version on PubMed Central for supplementary material.

Acknowledgments

We thank C. Doe, T. Hays, G. Rogers, S. Rogers, T. Uemura, A. Wodarz, the Bloomington Stock Center and DSHB for reagents; and B. Goldstein, G. Rogers, S. Rogers, N. Rusan and U. Tepass for critiques. This work was funded by NIH R01 GM47857 to M.P.T.H. was funded by NSERC and CIHR PDFs. T.H. is currently supported by a Tier II Canada Research Chair and NSERC and CIHR grants.

References

Bayraktar J, Zygmunt D, Carthew RW. Par-1 kinase establishes cell polarity and functions in Notch signaling in the Drosophila embryo. J Cell Sci 2006;119:711–721. [PubMed: 16449319]

Bertet C, Sulak L, Lecuit T. Myosin-dependent junction remodelling controls planar cell intercalation and axis elongation. Nature 2004;429:667–671. [PubMed: 15190355]

Bilder D, Schober M, Perrimon N. Integrated activity of PDZ protein complexes regulates epithelial polarity. Nat Cell Biol 2003;5:53–58. [PubMed: 12510194]

Blankenship JT, Backovic ST, Sanny JS, Weitz O, Zallen JA. Multicellular rosette formation links planar cell polarity to tissue morphogenesis. Dev Cell 2006;11:459–470. [PubMed: 17011486]

Cau J, Hall A. Cdc42 controls the polarity of the actin and microtubule cytoskeletons through two distinct signal transduction pathways. J Cell Sci 2005;118:2579–2587. [PubMed: 15928049]

Cox RT, Kirkpatrick C, Peifer M. Armadillo is required for adherens junction assembly, cell polarity, and morphogenesis during Drosophila embryogenesis. J Cell Biol 1996;134:133–148. [PubMed: 8698810]

Etienne-Manneville S, Hall A. Cdc42 regulates GSK-3beta and adenomatous polyposis coli to control cell polarity. Nature 2003;421:753–756. [PubMed: 12610628]

Fan S, Hurd TW, Liu CJ, Straight SW, Weimbs T, Hurd EA, Domino SE, Margolis B. Polarity proteins control ciliogenesis via kinesin motor interactions. Curr Biol 2004;14:1451–1461. [PubMed: 15324661]

Fehon R. Cell biology: polarity bites. Nature 2006;442:519–520. [PubMed: 16862127]

Gomes ER, Jani S, Gundersen GG. Nuclear movement regulated by Cdc42, MRCK, myosin, and actin flow establishes MTOC polarization in migrating cells. Cell 2005;121:451–463. [PubMed: 15882626]

Gumbiner BM. Regulation of cadherin-mediated adhesion in morphogenesis. Nat Rev Mol Cell Biol 2005;6:622–634. [PubMed: 16025097]

Harris TJ, Peifer M. Adherens junction-dependent and -independent steps in the establishment of epithelial cell polarity in Drosophila. J Cell Biol 2004;167:135–147. [PubMed: 15479740]

Harris TJ, Peifer M. The positioning and segregation of apical cues during epithelial polarity establishment in Drosophila. J Cell Biol 2005;170:813–823. [PubMed: 16129788]

Hurov JB, Watkins JL, Piwnica-Worms H. Atypical PKC phosphorylates PAR-1 kinases to regulate localization and activity. Curr Biol 2004;14:736–741. [PubMed: 15084291]

Hutterer A, Betschinger J, Petronczki M, Knoblich JA. Sequential roles of Cdc42, Par-6, aPKC, and Lgl in the establishment of epithelial polarity during Drosophila embryogenesis. Dev Cell 2004;6:845–854. [PubMed: 15177032]

Irvine KD, Wieschaus E. Cell intercalation during Drosophila germband extension and its regulation by pair-rule segmentation genes. Development 1994;120:827–841. [PubMed: 7600960]

Jamora C, Fuchs E. Intercellular adhesion, signalling and the cytoskeleton. Nat Cell Biol 2002;4:E101–108. [PubMed: 11944044]

Kemphues K. PARsing embryonic polarity. Cell 2000;101:345–348. [PubMed: 10830161]

Knox AL, Brown NH. Rap1 GTPase regulation of adherens junction positioning and cell adhesion. Science 2002;295:1285–1288. [PubMed: 11847339]

Lecuit T, Wieschaus E. Polarized insertion of new membrane from a cytoplasmic reservoir during cleavage of the Drosophila embryo. J Cell Biol 2000;150:849–860. [PubMed: 10953008]

Lemmers C, Michel D, Lane-Guermonprez L, Delgrossi MH, Medina E, Arsanto JP, Le Bivic A. CRB3 binds directly to Par6 and regulates the morphogenesis of the tight junctions in mammalian epithelial cells. Mol Biol Cell 2004;15:1324–1333. [PubMed: 14718572]

Ligon LA, Karki S, Tokito M, Holzbaur EL. Dynein binds to betacatenin and may tether microtubules at adherens junctions. Nat Cell Biol 2001;3:913–917. [PubMed: 11584273]

Muller HA, Wieschaus E. armadillo, bazooka, and stardust are critical for early stages in formation of the zonula adherens and maintenance of the polarized blastoderm epithelium in Drosophila. J Cell Biol 1996;134:149–163. [PubMed: 8698811]

Munro EM. PAR proteins and the cytoskeleton: a marriage of equals. Curr Opin Cell Biol 2006;18:86–94. [PubMed: 16364625]

Nance J. PAR proteins and the establishment of cell polarity during C. elegans development. Bioessays 2005;27:126–135. [PubMed: 15666355]

Nelson WJ. Adaptation of core mechanisms to generate cell polarity. Nature 2003;422:766–774. [PubMed: 12700771]

Ohno S. Intercellular junctions and cellular polarity: the PAR-aPKC complex, a conserved core cassette playing fundamental roles in cell polarity. Curr Opin Cell Biol 2001;13:641–648. [PubMed: 11544035]

Papoulas O, Hays TS, Sisson JC. The golgin Lava lamp mediates dynein-based Golgi movements during Drosophila cellularization. Nat Cell Biol 2005;7:612–618. [PubMed: 15908943]

Rolls MM, Albertson R, Shih HP, Lee CY, Doe CQ. Drosophila aPKC regulates cell polarity and cell proliferation in neuroblasts and epithelia. J Cell Biol 2003;163:1089–1098. [PubMed: 14657233]

Ruiz-Canada C, Ashley J, Moeckel-Cole S, Drier E, Yin J, Budnik V. New synaptic bouton formation is disrupted by misregulation of microtubule stability in aPKC mutants. Neuron 2004;42:567–580. [PubMed: 15157419]

Sotillos S, Diaz-Meco MT, Caminero E, Moscat J, Campuzano S. DaPKC-dependent phosphorylation of Crumbs is required for epithelial cell polarity in Drosophila. J Cell Biol 2004;166:549–557. [PubMed: 15302858]

Tabuse Y, Izumi Y, Piano F, Kemphues KJ, Miwa J, Ohno S. Atypical protein kinase C cooperates with PAR-3 to establish embryonic polarity in Caenorhabditis elegans. Development 1998;125:3607–3614. [PubMed: 9716526]

Tanentzapf G, Tepass U. Interactions between the crumbs, lethal giant larvae and bazooka pathways in epithelial polarization. Nat Cell Biol 2003;5:46–52. [PubMed: 12510193]

Tepass U. Crumbs, a component of the apical membrane, is required for zonula adherens formation in primary epithelia of Drosophila. Dev Biol 1996;177:217–225. [PubMed: 8660889]

Tepass U, Hartenstein V. The development of cellular junctions in the Drosophila embryo. Dev Biol 1994;161:563–596. [PubMed: 8314002]

Tepass U, Tanentzapf G, Ward R, Fehon R. Epithelial cell polarity and cell junctions in Drosophila. Annu Rev Genet 2001;35:747–784. [PubMed: 11700298]

Warn RM, Warn A. Microtubule arrays present during the syncytial and cellular blastoderm stages of the early Drosophila embryo. Exp Cell Res 1986;163:201–210. [PubMed: 3943561]

Wiggin GR, Fawcett JP, Pawson T. Polarity proteins in axon specification and synaptogenesis. Dev Cell 2005;8:803–816. [PubMed: 15935771]

Wodarz A. Molecular control of cell polarity and asymmetric cell division in Drosophila neuroblasts. Curr Opin Cell Biol 2005;17:475–481. [PubMed: 16099639]

Zallen JA, Wieschaus E. Patterned gene expression directs bipolar planar polarity in Drosophila. Dev Cell 2004;6:343–355. [PubMed: 15030758]

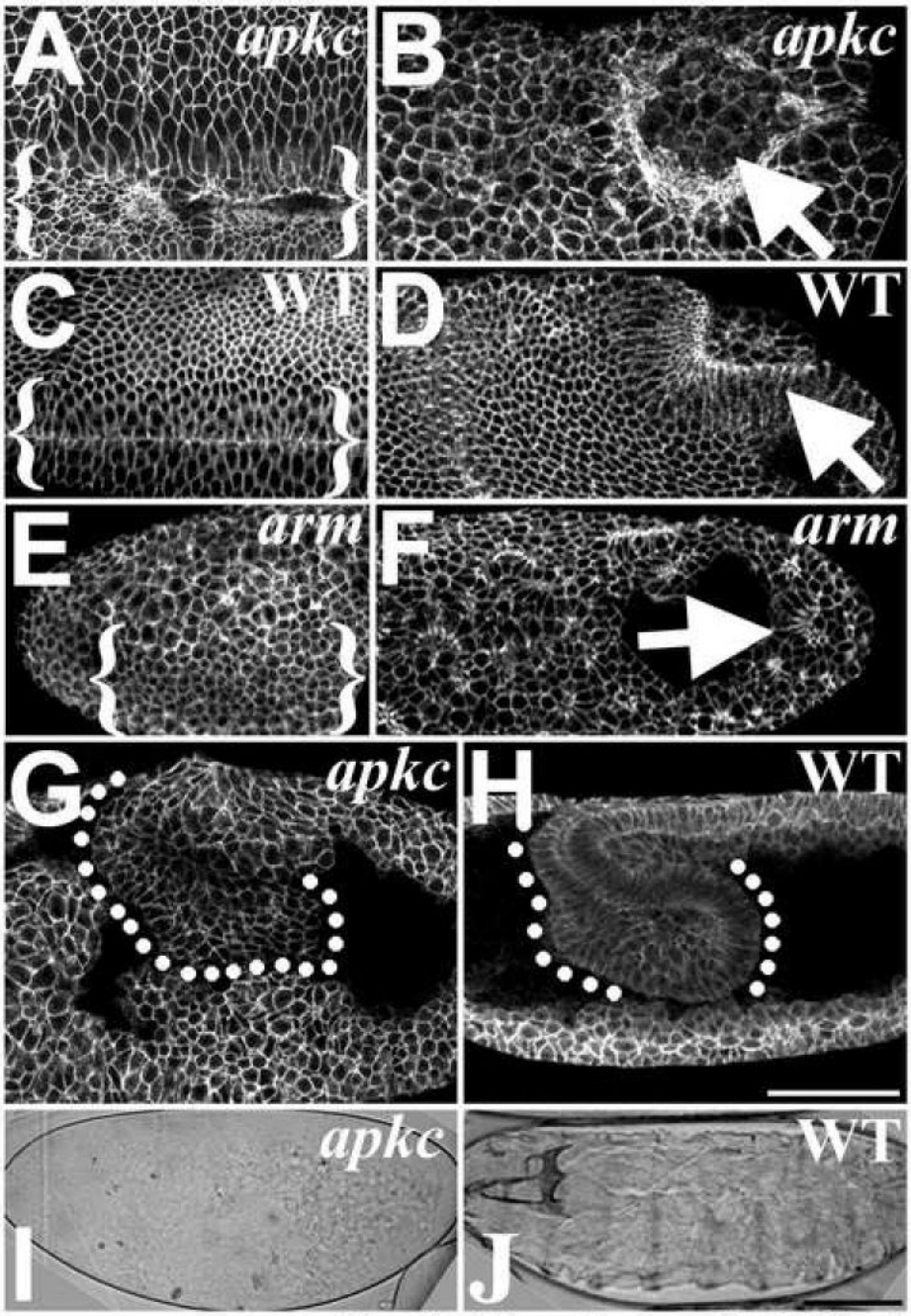

Figure 1. *apkc*$^{m/z}$ mutants gastrulate but display progressive epithelial breakdown

(A-H) Dlg labels cell cortexes. (A) *apkc*$^{m/z}$ mutant and (C) WT ventral furrows (bracketed). (B) *apkc*$^{m/z}$ mutant and (D) WT posterior midgut invaginations (arrows). (E) *arm*$^{m/z}$ mutant ventral furrow (bracketed; furrow identified by Twist staining (data not shown)). (F) *arm*$^{m/z}$ mutant posterior midgut invagination (arrow; embryo oriented by Miranda staining (data not shown)). The epithelium forms balls as it breaks down. (G) *apkc*$^{m/z}$ mutants undergo germband extension but then display widespread epithelial dissociation and cell rounding versus WT (H). (I) *apkc*$^{m/z}$ mutant cuticle—note small scraps of cuticle secreted from remaining epithelial cells. (J) WT. Bars, 50μm.

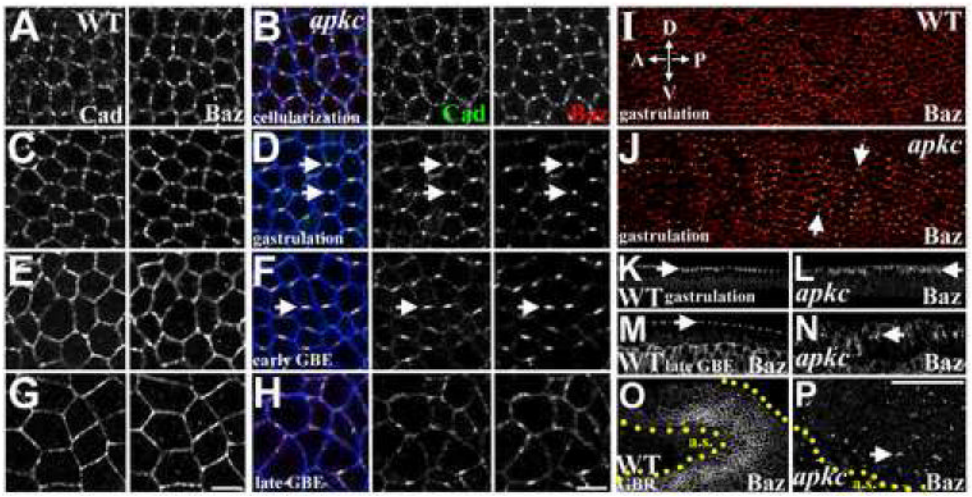

Figure 2. AJs and Baz lose symmetry and form abnormal planar-polarized puncta during *apkc* mutant gastrulation

(A-H) DE-Cad, green. Baz, red. Dlg, blue, marks plasma membrane. (A) WT cellularization. DE-Cad and Baz colocalize in spot junctions evenly distributed around the apical periphery. (B) Cellularizing *apkc*$^{m/z}$ mutant. DE-Cad and Baz are indistinguishable from WT (A). (C) Early WT gastrulation. DE-Cad and Baz remain in uniformly distributed spot junctions. (D) Early *apkc*$^{m/z}$ mutant gastrulation (ventral furrow formation). DE-Cad and Baz form puncta located centrally along the dorsal and ventral sides of each cell (arrows). (E) Early WT germband extension. Spot junctions begin coalescing. DE-Cad and Baz colocalize around full apical periphery. (F) Early *apkc*$^{m/z}$ mutant germ band extension. Planar-polarized DE-Cad/Baz puncta maintained. (G) Late WT germband extension. DE-Cad and Baz uniformly distributed. (H) Late *apkc*$^{m/z}$ mutant germ band extension. DE-Cad/Baz puncta lose planar polarity and become disorganized. (I, J) Planar-polarized DE-Cad/Baz puncta throughout the epithelium at gastrulation (J), in contrast to the symmetric WT distribution (I) (Baz shown in glow scale). (K) WT gastrulation. Baz localizes apically just below the apex of each cell (arrow). (L) *apkc*$^{m/z}$ mutant gastrulation. Baz localizes apically below the apex of each cell (arrow). (M) WT late germ band extension. Baz localizes around the apex of each epithelial cell (M, side view, arrow; O, surface view, next to amnioserosa cells (a.s.). (N) Late *apkc*$^{m/z}$ mutant germ band extension. Baz localizes more basally (N, side view, arrow) in fragmented complexes (P, surface view, arrow). Bars, 5μm (A-H), 50μm (I-P).

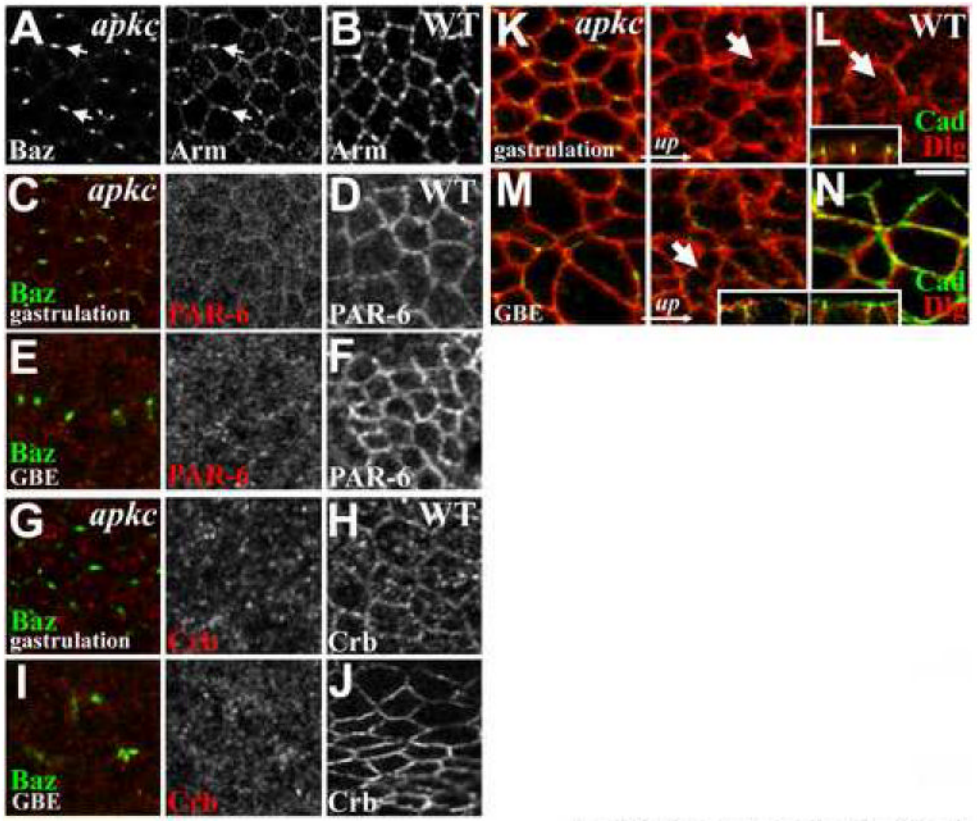

Figure 3. aPKC's effects on polarity cues

(A) Arm colocalizes with Baz in puncta in gastrulating *apkc*$^{m/z}$ mutants (arrows). (B) Arm in WT spot junctions. (C) Lack of PAR-6 and (G) Crb enrichment at Baz puncta in gastrulating *apkc*$^{m/z}$ mutants. Both have reduced cortical enrichment at both gastrulation (C, G) and after germband extension (E, I) versus WT (D, F, H, J). (K) Dlg overlaps with DE-Cad puncta in gastrulating *apkc*$^{m/z}$ mutants and localizes to apical surface membrane (arrow), as in WT (L, arrow; inset shows a side view at this stage). (M) Dlg continues to localize to apical surface membrane after *apkc*$^{m/z}$ mutant germband extension (arrow; inset shows a side view at this stage), in contrast to WT where Dlg localizes below DE-Cad (N, a slightly oblique section in which the top of the panel is above the embryo surface; inset shows a side view at this stage). Bar, 5μm.

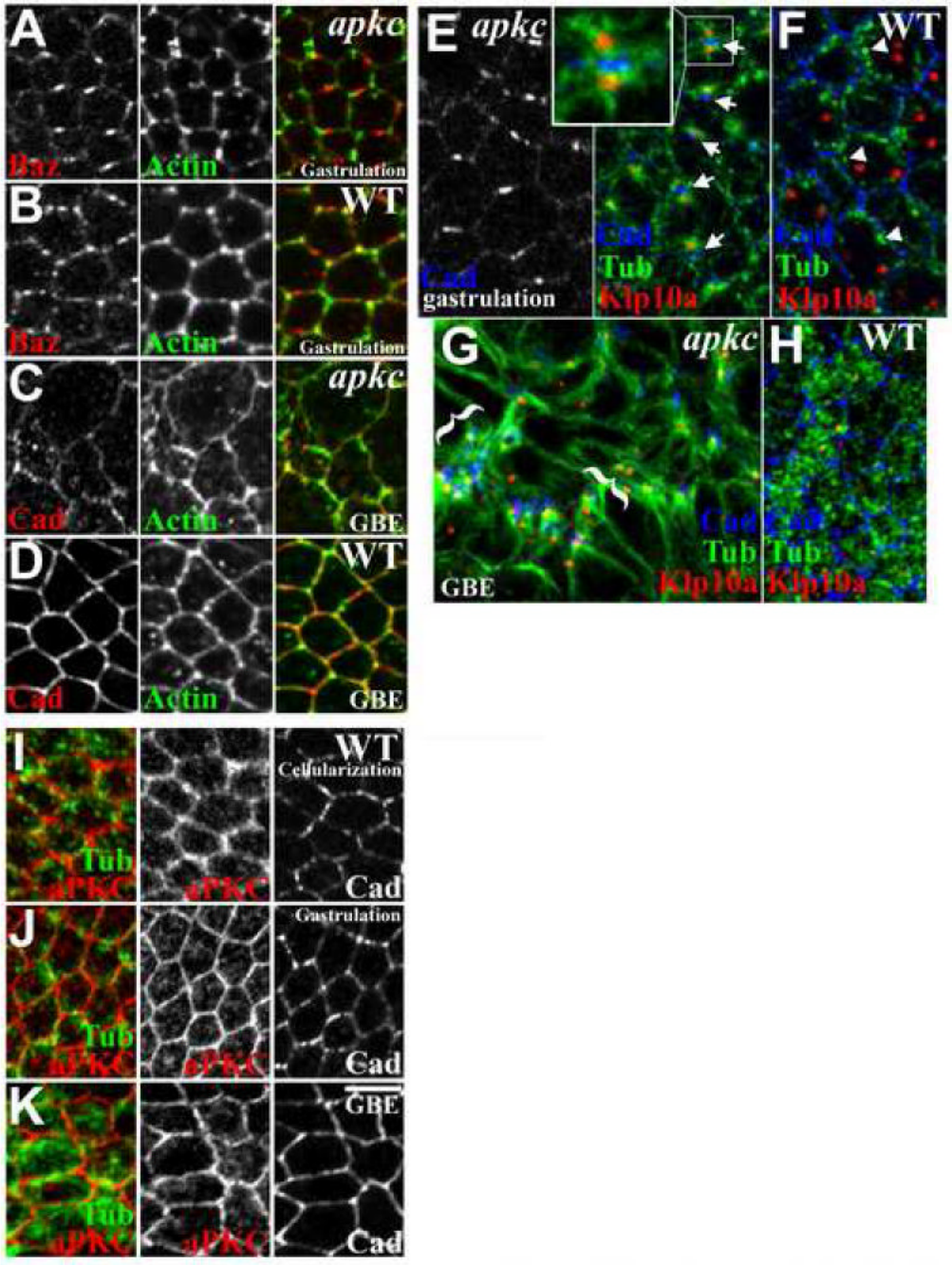

Figure 4. The *apkc*$^{m/z}$ mutant Baz/DE-Cad puncta associate with abnormal MT asters

(A) Actin is not specifically enriched in the abnormal puncta in gastrulating *apkc*$^{m/z}$ mutants, but is enriched in tricellular junctions, more than WT (B). (C) Actin staining reveals greater apical cell protrusions after *apkc*$^{m/z}$ mutant germband extension, in contrast to WT (D). (E) Asters of MTs (green) emanating from centrosomes (red, Klp10a) localize to either side of the planar-polarized DE-Cad puncta (blue) in gastrulating *apkc*$^{m/z}$ mutants. (F) WT MTs (green) form lateral bundles with minimal centrosome (red) association or planar polarity. (G) Centrosomal MTs localize next to AJ fragments after *apkc*$^{m/z}$ mutant germband extension (bracketed), in contrast to WT (H). (I-K) WT localization of aPKC (red) relative to MTs (green)

and AJs (right) at cellularization (I), gastrulation (J) and during germband extension (K) (at each stage the samples are triple stained and imaged in the same plane). Bar, 5μm.

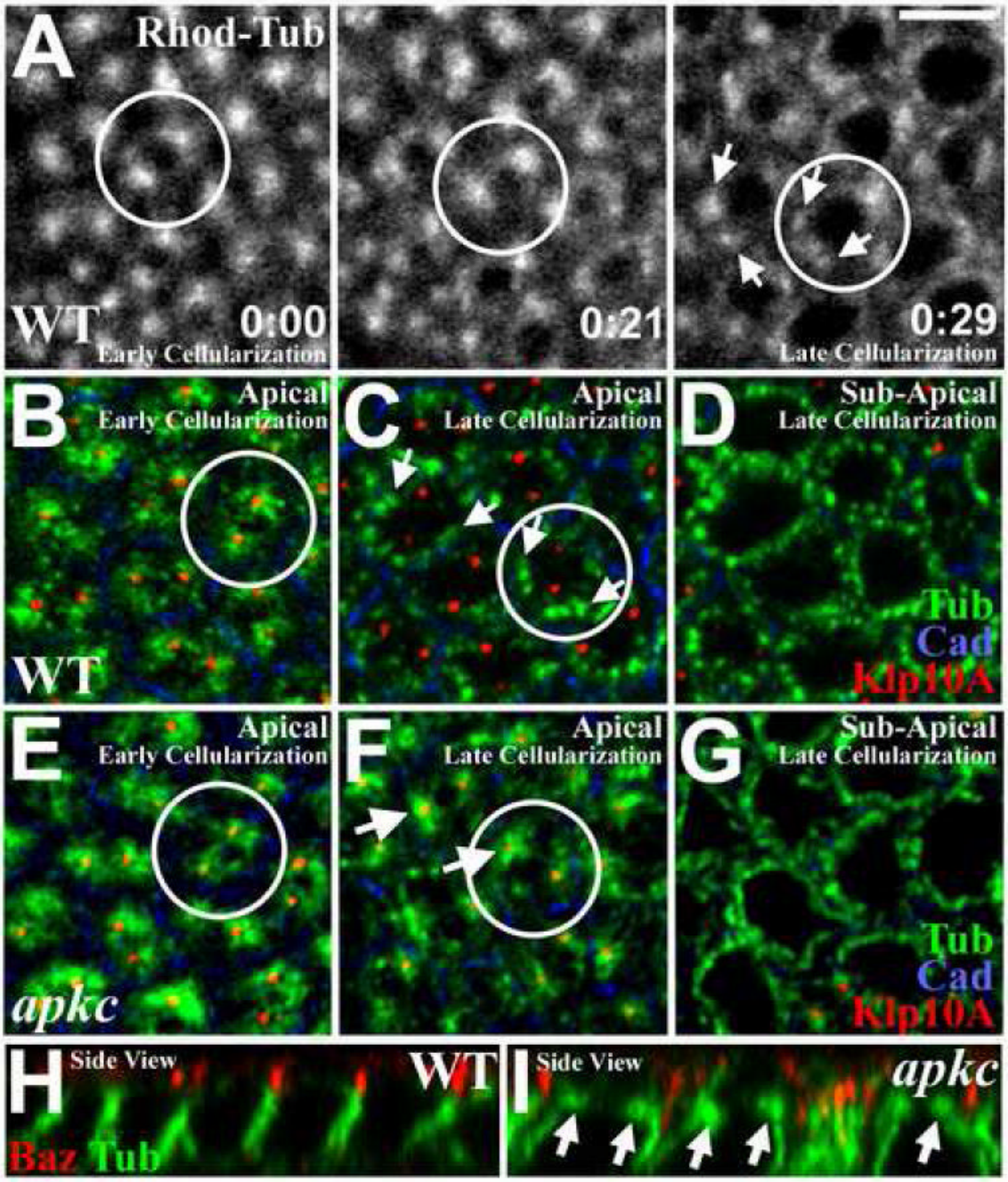

Figure 5. MT asters are not released from centrosomes during *apkc* mutant cellularization

(A) Live imaging of WT embryos injected with rhodamine-labeled tubulin, focusing on apical MTs. Early cellularization (0:00, h:min): MTs form two apical asters per cell compartment. By late cellularization (0:29): apical asters break into MT bundles (arrows) running basally down the lateral membranes. (See Video 1) (B) Early WT cellularization. Apical MTs (green) are closely associated with two apical centrosomes (marked with Klp10a (red)) per cell compartment (plasma membrane: DE-Cad (blue)). (C) Late WT cellularization. Apical MTs (green) dissociate from centrosomes (red; arrows). (D) Imaging just basal to plane in (C) reveals lateral MT bundles in cross-section (green). (E) Early *apkc*$^{m/z}$ mutant cellularization. Apical MTs (green) associate with apical centrosomes (Klp10a (red)) as in WT (B). (F) Late

apkc$^{m/z}$ mutant cellularization. MT asters (green) remain associated with centrosomes (red). (G) Imaging just basal to plane in (F) reveals lateral MT bundles in cross-section (green). (H) Side view, late WT cellularization. Note loss of apical MT asters. (I) Side view, late *apkc*$^{m/z}$ mutant cellularization. Note abnormal persistence of apical MT asters. Bar, 5μm.

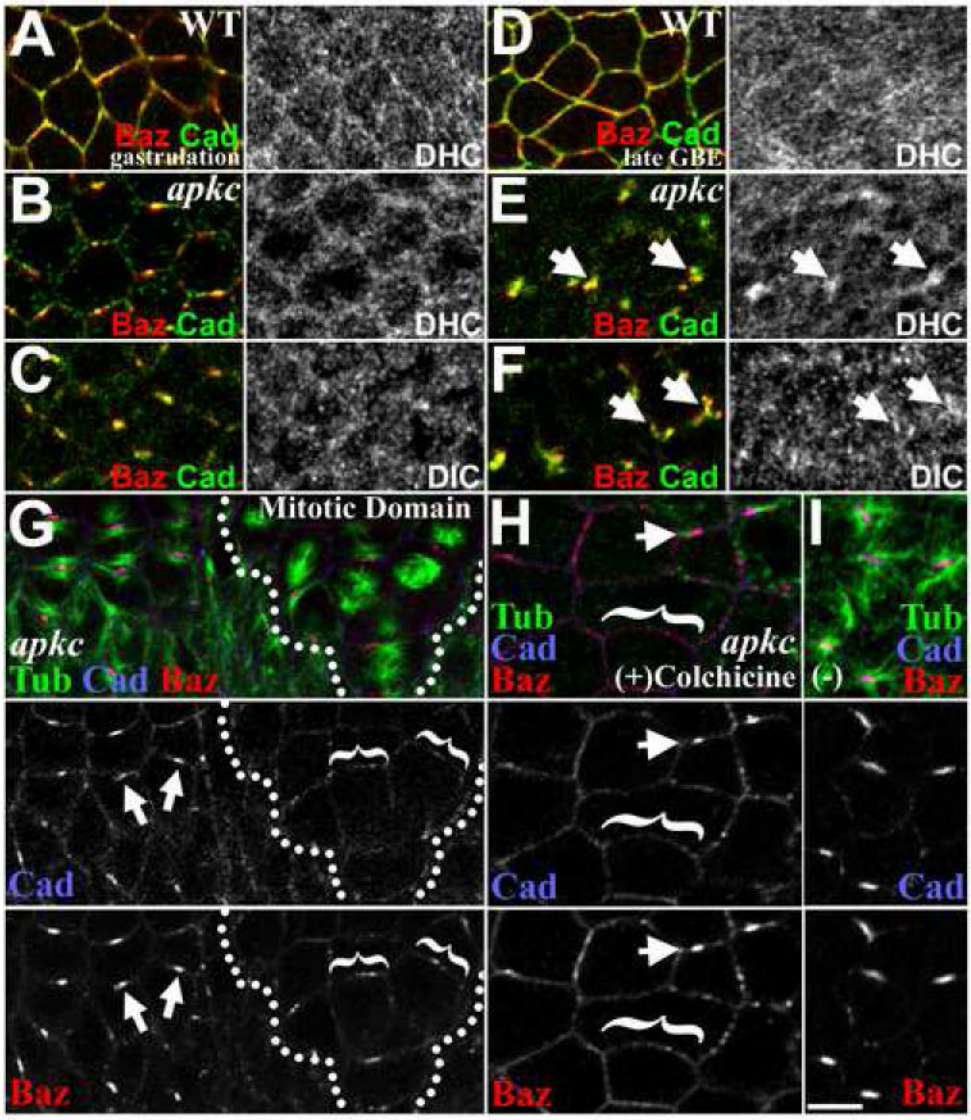

Figure 6. The roles of Dynein and MTs in AJ clustering in *apkc*$^{m/z}$ mutants

(A) During WT gastrulation, Dynein heavy chain has an even cytoplasmic distribution with some enrichment at the cortex in proximity to AJs and Baz (Dynein intermediate chain has a similar distribution (data not shown)). (B, C) During *apkc*$^{m/z}$ mutant gastrulation, both Dynein heavy chain (B) and Dynein intermediate chain (C) have even cytoplasmic and cortical distributions. (D) At full WT germband extension, the Dynein distribution remains even. (E, F) At full *apkc*$^{m/z}$ mutant germband extension, Dynein heavy chain (E) and Dynein intermediate chain (F) show specific enrichment at fragmented AJ/Baz complexes (arrows). (G-I) *apkc*$^{m/z}$ mutants, DE-Cad (blue), Baz (red), MTs (green). (G) DE-Cad/Baz puncta disperse as MTs (blue) are lost from the cortex when spindles form in the first mitotic domains (compare mitotic cells, left (dispersing complexes bracketed), with cells yet to divide, right (arrows, intact complexes)). (H) Colchicine-treatment (30 min) of gastrulating *apkc*$^{m/z}$ mutants induces MT (blue) loss in most cells and a corresponding dispersion of DE-Cad/Baz puncta (bracketed). Arrows, complexes retained in cells with residual MTs. (I) Ethanol carrier alone. Bar, 5 μm.

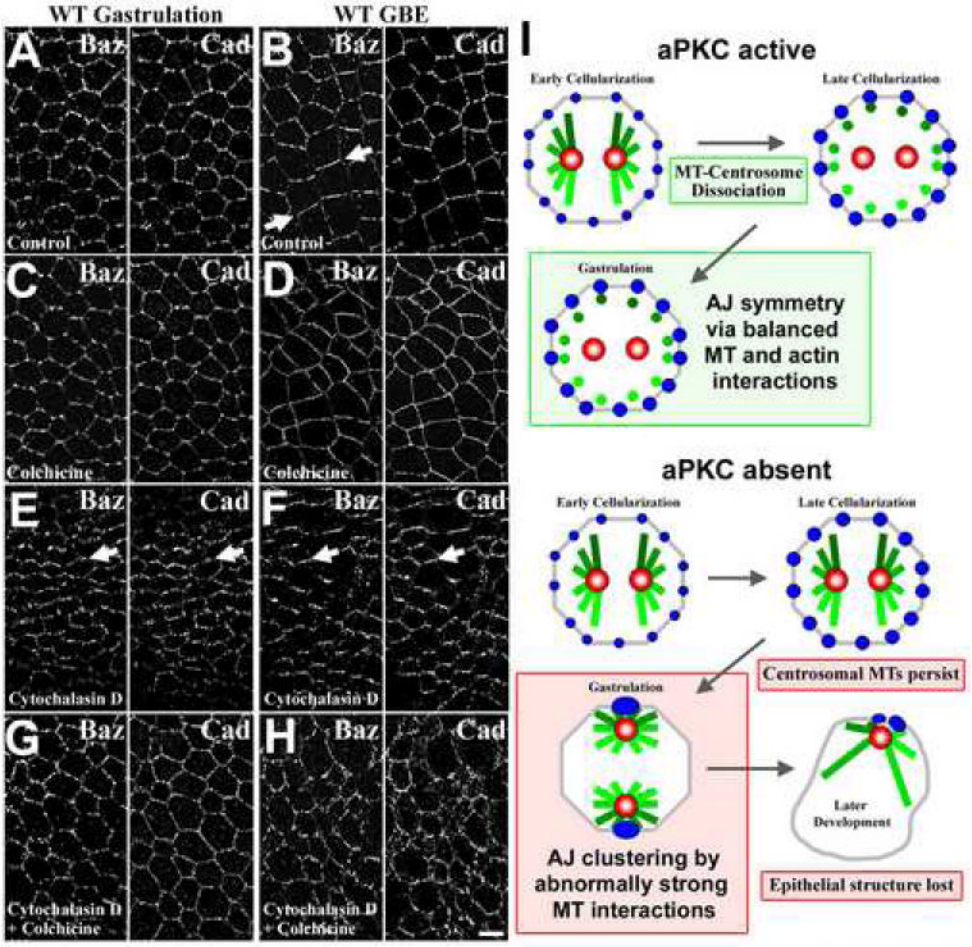

Figure 7. Coordinated cytoskeletal activity and the symmetry of Baz/AJs positioning

Projections of deconvolved confocal stacks of WT embryos at gastrulation (A, C, E, G) and during germband extension (B, D, F, H) are shown. (A, B) Treatment with carrier alone had no effect on Baz/AJ (DE-Cad) positioning. Baz develops some planar polarity (arrow). (C, D) Disruption of MTs with colchicine had minimal effects of Baz/AJ positioning. (E, F) Disruption of actin with cytochalasin D produced enhanced planar polarity of both Baz and DE-Cad at both stages. (G, H) Simultaneous treatment with cytochalasin D and colchicine resulted in a relatively symmetric distribution of Baz and DE-Cad at both stages. Bar, 5 μm. (I) A model of aPKC regulation of MT organization, AJ positioning and epithelial structure during development.